small
NANO MICRO

Probing the Effect of Molecular Orientation on the Intensity of Chemical Enhancement Using Graphene-Enhanced Raman Spectroscopy

*Xi Ling, Juanxia Wu, Weigao Xu, and Jin Zhang**

A rational approach to investigate the effect of molecular orientation on the intensity of chemical enhancement using graphene-enhanced Raman spectroscopy (GERS) is developed. A planar molecule, copper phthalocyanine (CuPc), is used as probe molecule. Annealing allows the CuPc molecule in a Langmuir–Blodgett film to change orientation from upstanding to lying down. The UV–visible absorption spectra prove the change of the molecular orientation, as well as the variation of the interaction between the CuPc molecule and graphene. The Raman spectra of the molecule in the two different orientations are compared and analyzed. The results show that chemical enhancement is highly sensitive to the molecular orientation. The different molecular orientations induce different magnitudes of the interaction between the molecule and graphene. The stronger the interaction, the more the Raman signal is enhanced. Furthermore, the sensitivity of GERS to molecular orientation is promising to determine the orientation of the molecule on graphene. Based on this molecular orientation sensitive Raman enhancement, quantitative calculation of the magnitude of the chemical enhancement is implemented for a series of Pc derivatives. It shows that the magnitude of the chemical enhancement can be used to evaluate the degree of interaction between the molecules and graphene. Moreover, an understanding of the chemical enhancement in GERS is promoted and the effect of molecular orientation on the intensity of chemical enhancement is explained.

1. Introduction

Due to the ultrahigh sensitivity and molecular specificity, surface-enhanced Raman spectroscopy (SERS) has been developed as one of the most promising techniques among various spectroscopic methods.[1] Even though SERS was discovered in the 1970s and single-molecule-sensitive detection was realized in 1997,[2] there is still a long way to practical applications since this technique has many challenges.[3] One of the most important problems is the controversy about its enhancement mechanism. Since the very beginning when SERS was put forward, an electromagnetic mechanism (EM)[4] and chemical mechanism (CM)[5–7] were considered as two widely accepted processes among the controversial mechanisms of SERS. These two mechanisms usually coexist in a traditional SERS substrate based on a rough metal surface. Due to the huge enhancement of the EM compared to the minor enhancement of the CM, the contribution of the CM is usually covered up by the EM, which largely limits the investigation of the CM.[8–10] Thus, the understanding of the CM is more ambiguous that that of the EM. To isolate

X. Ling, J. X. Wu, W. G. Xu, Prof. J. Zhang
Center for Nanochemistry
Beijing National Laboratory for Molecular Sciences
Key Laboratory for the Physics and
Chemistry of Nanodevices
State Key Laboratory for Structural Chemistry
of Unstable and Stable Species
College of Chemistry and Molecular Engineering
Peking University
Beijing 100871, P.R. China
E-mail: jinzhang@pku.edu.cn

DOI: 10.1002/smll.201102223

the CM from EM, the best way is to choose an enhancement system where there is only a CM. In our previous work, graphene-enhanced Raman spectroscopy (GERS) was discovered, and a systematic investigation and analysis were carried out. This led us to believe that the GERS system is an ideal system in which there is only a CM that suffers no EM disturbances.[11–14] Therefore, GERS provides a convenient system for investigating the issues of the CM.

The most common situation in molecular spectroscopy is the measurement of an ensemble of many randomly oriented molecules. This infers that the signal is normally an average result.[15] The molecular orientation dependence of SERS has been thought to be an important but complex issue for a long time.[16–20] The molecular orientation influences not only the polarization of the local electromagnetic field, but also the interaction state between the molecule and the substrate. In a traditional SERS system, the enhancement is mainly based on the "hot spot" site. It is difficult to control and confirm the molecular orientation of single or few molecules on this site.[21–24] Besides, the inhomogeneity of the substrate magnifies this problem. Meanwhile, the molecular orientation influences both the EM and CM, and it is difficult to determine an accurate relationship between molecular orientation and the EM or CM. For these reasons, to study the molecular orientation dependence of SERS, one should consider the following aspects: 1) a flat surface with uniform sites where a uniform molecular orientation can form easily; and 2) the large number of molecules with unified orientation under the laser point, which permits the observation of Raman signals from one special molecular orientation.

Graphene is a perfect 2D material with a monolayer of carbon atoms packed into a honeycomb crystal plane, which is uniform and was previously reported to play a role as a Raman enhancement substrate.[11,25] Molecules can easily form a unified orientation collectively on it due to the flatness of the surface. This allows measurement of the Raman signal from molecules with a unified orientation, rather than an average effect from many randomly oriented molecules. Graphene enlarges the molecular orientation change and makes this effect easier to observe. Moreover, one advantage of GERS is that there is only chemical enhancement, which indicates that the change of the molecular orientation would change only the contribution from the chemical enhancement, with no electromagnetic enhancement disturbance. Therefore, the GERS system is a superior candidate for investigating the effect of molecular orientation on the intensity of the chemical enhancement.

2. Results and Discussion

2.1. Variation of the Raman Intensity of Copper Phthalocyanine Film after Annealing at Different Temperatures

Graphene was obtained by mechanical exfoliation on a 300 nm SiO_2/Si substrate. An upstanding copper phthalocyanine (CuPc) layer was constructed on top of graphene using the Langmuir–Blodgett (LB) technique.[26] A surface pressure (π) versus occupied molecular area (A) isotherm was obtained at a constant compression speed of 2 mm min^{-1} after allowing 30 min for complete evaporation of the solvent. Monolayer transfer onto the substrate was performed at π = 20 mN m^{-1} by a horizontal dipping method. From the π–A curve of the CuPc LB film, the obtained limiting area per molecule is about 0.52 nm^2 which indicates that the CuPc molecules are in a configuration with a tilt angle of about 72°.[27] Again, the atomic force microscopy (AFM) image shows that the CuPc LB film is homogeneously arranged and cross-sectional analysis shows that the height of the LB film is about 1.5 nm (see Part 1 in the Supporting Information). Upon annealing the above sample, the CuPc molecule prefers to take a lying-down conformation on graphene, since the lying-down orientation is a stable orientation in both thermodynamics and dynamics equilibrium because of the similarity of the structure of the CuPc molecule and graphene.[28,29] As illustrated in **Figure 1**, after annealing the CuPc LB film on graphene, the orientation of the CuPc molecule changes from upstanding to lying down. Meanwhile, during the annealing process, it should be noted that not only can the molecular orientation change from upstanding to lying down, but also the number of molecules will decrease due to the lack of space. At a certain temperature, after desorption of some redundant molecules due to the limited space, all of the molecules left on graphene will be lying down and covering the graphene surface completely. Based on this reasonable assumption, a quantitative calculation of the chemical enhancement will be implemented later.

Next, an appropriate annealing temperature was found by investigating several temperatures. The sample was annealed in a 300 sccm (standard-state cubic centimeter per minute) Ar atmosphere for 10 min at a series of temperatures from room temperature to 600 °C with increments of 50 °C. The corresponding series of Raman spectra are shown in Part 2 of the Supporting Information. **Figure 2**a and b show a comparison of the Raman spectra of as-prepared CuPc LB

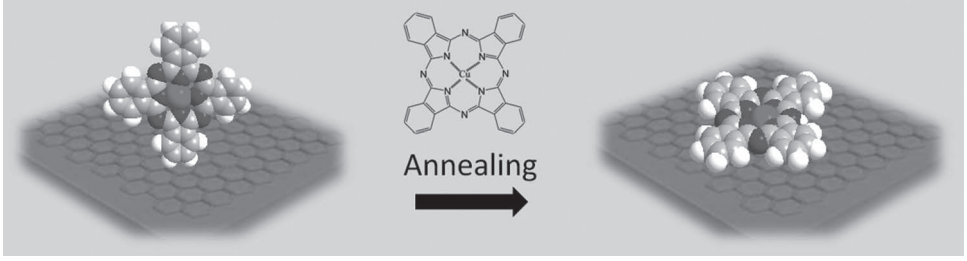

Figure 1. Schematic illustration of molecular orientation change under annealing. Inset: the molecular structure of CuPc.

NANO MICRO small

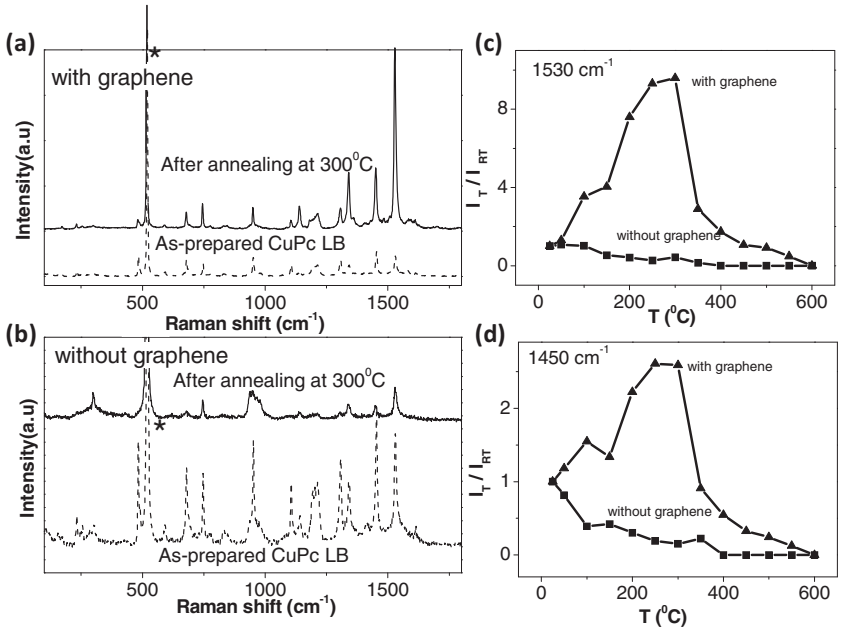

Figure 2. a) Comparison of Raman spectra of as-prepared CuPc LB film (dashed line) and that after annealing at 300 °C (solid line) on an SiO_2/Si substrate with graphene. b) Similar to (a) but without graphene. c,d) Curves of the relative Raman intensity after annealing (I_T) as a function of the annealing temperature, normalized by the Raman intensity of as-prepared CuPc LB film at room temperature (I_{RT}). Peaks at 1530 and 1450 cm^{-1} are taken as references in (c) and (d), respectively.

film and the film after annealing at 300 °C; considering the series of UV–vis absorption spectra and the AFM images in **Figure 3** and **4**, in which the data is analyzed later, an optimum temperature is around 300 °C since the remaining CuPc molecules are lying down and completely covering the graphene surface. Figure 2a corresponds to CuPc molecules on an area with graphene, while Figure 2b corresponds to an area without graphene. Interestingly, the Raman intensity of the CuPc molecules on graphene was enhanced significantly after annealing, whereas it decreased for the CuPc molecules on the area without graphene. Figure 2c and d show the variation of the Raman intensity of the peaks at about 1530 and 1450 cm^{-1} as a function of the annealing temperature, where the 1530 cm^{-1} mode was assigned to the symmetric stretching motion of isoindole groups and the 1450 cm^{-1} mode was assigned to the deformation of the isoindole ring system.[30] For the area with graphene (triangular symbols), the Raman intensity is the strongest when annealing at 300 °C, and the Raman signals can be well distinguished even after annealing at 550 °C. Moreover, the Raman intensity of peak 1530 cm^{-1} after annealing at 500 °C is comparable to that of as-prepared CuPc LB film, even though the number of molecules is obviously reduced after annealing. Besides, for different vibrational bands, their enhancement behaviors perform differently. As illustrated in Figure 2c and d, the two peaks at 1530 and 1450 cm^{-1} are enhanced tenfold and threefold, respectively. However, for the area without graphene (square symbols), all the peaks decrease gradually and the signals are invisible after annealing at 400 °C or higher.

2.2. UV–Visible Absorption Spectroscopy Characterization and Determination of the Variation of the Molecular Orientation on Graphene

UV–visible absorption spectroscopy was also used to investigate this process, which was a useful way to investigate the interaction between two species.[31] For phthalocyanines, the UV–visible absorption spectrum is observed from molecular orbitals within the aromatic 18π-electron system and from overlapping orbitals on the central metal atom. The two well-known bands of phthalocyanine derivatives in the UV–visible absorption spectra are the Soret (B) band in the region between 200 and 350 nm and the Q band in the region between 550 and 750 nm.[32] The Q band in the visible region has generally been interpreted in terms of π–π* excitation between bonding and antibonding molecular orbitals, and it usually splits into two peaks. The intense absorption band at about 628 nm (named Q1) was attributed to the aggregated species, due to face-to-face stacking of the CuPc molecule. The weak shoulder absorption at about 697 nm (named Q2) was assigned to the monomeric species.[27,33,34]

For measuring UV–visible absorption spectra, graphene was grown by the chemical vapor deposition (CVD) method on a copper foil and transferred onto a quartz substrate.[35] Then, the monolayer CuPc LB film was transferred onto the above substrate. For as-prepared CuPc LB film, as shown in Figure 3 (solid line), the UV–visible absorption spectrum shows the characteristic Soret band and Q band. The band at about 270 nm in Figure 3a represents the typical absorption of graphene. Before annealing, no matter whether there is graphene or not on the quartz substrate, the shape of the observed Q band is the same, with an intense absorption at about 628 nm and a weaker shoulder at about 696 nm. After annealing, the situation is entirely different in the Q-band region. As shown in Figure 3c, for film with graphene, the relative intensity of the two absorption bands in the Q-band region is opposite to that observed before. The Q1 band becomes weaker and broader, while the Q2 band becomes much stronger. The ratio of the absorption of Q2 and Q1 changes from 0.9 to 1.9. This indicates that the proportion of the aggregated species and monomeric species becomes smaller and larger, respectively. Therefore, we conclude that the molecular orientation changed from upstanding to lying down on graphene after annealing.

Meanwhile, the shift of the Q2 band from 696 to 704 nm is indicative of the decrease of the π–π* excitation energy, which is attributed to the stronger interaction between the CuPc molecule and graphene. For Pc derivatives, the Q band is from the highest filled a_{1u} orbital to the lowest unfilled e_g orbital, and the highest occupied molecular orbital (HOMO)

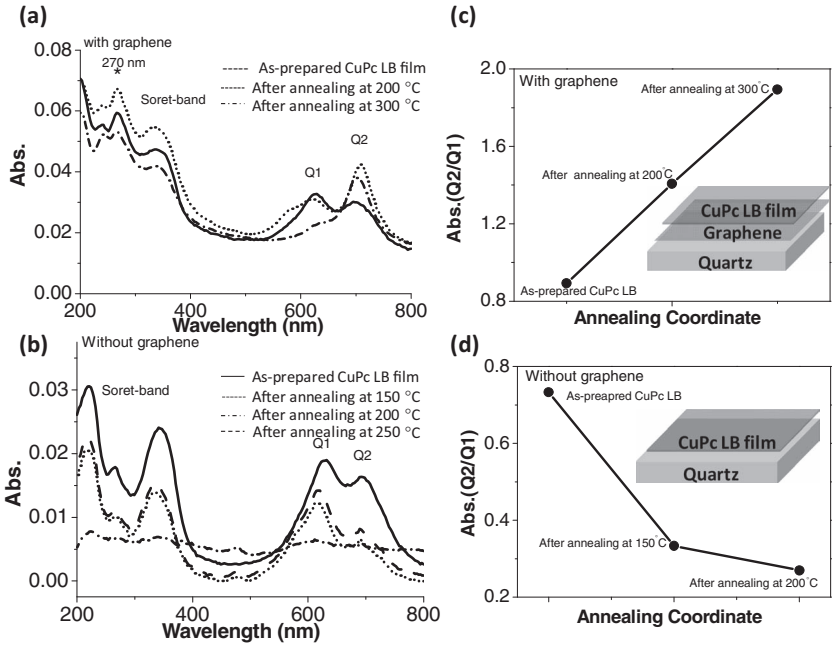

Figure 3. Comparison of the UV–visible absorption spectra of as-prepared CuPc LB film and that after annealing: a) with graphene; b) without graphene. c,d) Curves of the ratio of absorption of the Q1 and Q2 bands as a function of the annealing coordinate. The insets in (c) and (d) show schematic illustrations of the the corresponding sample structures.

is composed of the π electrons located on the Pc ring (a_{1u}).[36] Hence, the combination of graphene and the CuPc molecule decreased the energy gap between the a_{1u} orbital and the e_g orbital and consequently decreased the π–π^* excitation energy. It should also be noted that the absorption at 632.8 nm is decreased after annealing, where 632.8 nm is the excitation wavelength of the Raman measurement. This indicates that the Raman enhancement after annealing in Figure 2a is not due to the enhancement of the absorption cross section. However, for film without graphene, as shown in Figure 3b and d, the absorption of the Q1 band is always larger than that of the Q2 band during the annealing program. The relative intensity of the two absorption bands in the Q-band region changes very little, just an entire decrease of the absorption due to the decrease of the number of molecules, and the absorption is undetectable when the annealing temperature is higher than 250 °C. After annealing at 200 °C, the Q1-band absorption changed from 0.024 to 0.014, which indicated that the number of molecules decreased to 0.58 times that of the as-prepared CuPc LB film. Besides, different from that with graphene, the Q band shifts to a high-energy direction, which is due to the change of the crystal form.[32] Hence, the change of the UV–visible absorption spectra in Figure 3a is strongly related to graphene, which indicates not only the change of the molecular orientation from upstanding to lying down, but also that the π–π interaction between the CuPc molecule and graphene is stronger.

In addition, by combining the series of AFM images shown in Figure 4, it is not difficult to speculate about the state of the molecules on the substrate during the annealing process. When annealing at low temperature, such as 150 °C, the uniform CuPc LB film becomes rough and some CuPc molecules aggregate to form particles. Cross-sectional analysis showed the increase of the roughness of the surface. This is as a result of some molecules changing from upstanding to lying-down orientation. Meanwhile, the temperature is not high enough for desorption of the molecules, and there is not enough space for all of the molecules, hence the redundant molecules aggregate to

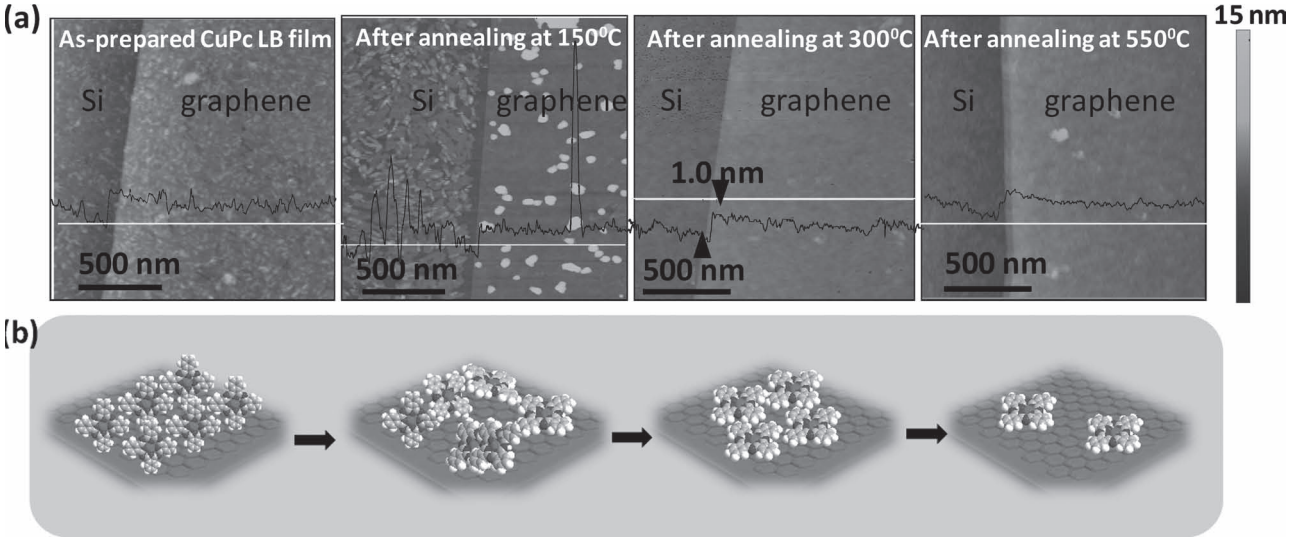

Figure 4. a) Series of AFM images of CuPc LB film after annealing at different temperatures. The insets show the cross-sectional analysis of the AFM images. All of the height profiles are on the same scale. b) Corresponding schematic illustrations of the molecules on the substrate.

NANO MICRO small

form particles. When annealing at higher temperature, such as 300 °C, which is near the sublimation temperature of the CuPc molecules, most of the molecules are desorbed from the substrate. However, due to the strong π–π interaction between the lying-down CuPc molecules and graphene, the first-layer molecule in contact with graphene will be the most difficult to desorb, and it remains on the graphene surface. Hence, the AFM image after annealing at 300 °C looks very smooth. It is these remaining molecules that have a large contribution to the Raman intensity as shown in Figure 2a. By raising the annealing temperature further, the thermal energy overcomes the π–π interaction between the CuPc molecules and graphene. Thus, the CuPc molecules are desorbed, which results in a decrease in Raman intensity. The AFM images after annealing at 300 and 550 °C show that the molecules have a similar surface flatness, since the isolated lying-down CuPc molecules are difficult to distinguish by AFM. As analyzed above, it is easy to understand the decrease of the Raman intensity in Figure 2b, as a result of the decrease of the total number of molecules. However, the situation is more complex for Figure 2a. Due to the existence of graphene, the GERS effect cannot be neglected here. Besides the decrease of the number of molecules, molecular orientations from upstanding to lying down influence the Raman intensity greatly. The former was known to decrease the Raman intensity, which indicated the latter enhanced it more remarkably since we observed the enhancement effect after annealing, as shown in Figure 2a. Note that when there is no other enhancement effect, annealing of the CuPc LB film will simply induce a decrease of the Raman intensity.[37,38] Therefore, we conclude here that the Raman intensity in GERS is very sensitive to the molecular orientation. Meanwhile, the molecular orientation sensitivity of the CM was well expressed in GERS, which was usually ignored in traditional SERS where the EM dominated the final SERS signal (see Part 3 in the Supporting Information).

To confirm the origin of the observed enhancement further, a control experiment based on solution soaking deposition of the CuPc molecule was carried out (see Part 4 in the Supporting Information), which results in a pristine lying-down orientation on graphene.[39] Annealing at temperatures below 300 °C will not change the Raman intensity, as shown in Figure S4, because the molecular orientation as well as the number of CuPc molecules does not change. They always keep the lying-down orientation on graphene no matter whether before or after annealing. Moreover, the relative Raman intensity of the CuPc molecules deposited by solution soaking is the same as that of CuPc LB film after annealing, but different from the as-prepared CuPc LB film (see Figure S5a). Besides, both of them have similar UV–visible absorption spectra with the Q2 band stronger than the Q1 band (see Figure S5b). This indicates that the CuPc LB film after annealing has the same CuPc molecular orientation as the CuPc deposited on graphene by solution soaking. Both of them adopt the lying-down orientation. In addition, the results imply the enhancement in Figure 2a originates from the change from upstanding to lying-down molecular orientation.

2.3. Understanding the Chemical Mechanism and Molecular Orientation Sensitivity in GERS

As for the traditional understanding of the chemical enhancement, it has been attributed to charge-transfer excitation between the substrate and the adsorbate. It is usually thought of as a resonant Raman type due to the change of resonance condition that is more matched with the excitation laser. However, in this work, the opposite performance of the absorption at 632.8 nm in Figure 3a and the Raman intensity in Figure 2a indicates that there is another factor dominating the Raman scattering cross section other than the resonance condition. Actually, the origin of the Raman enhancement is the magnitude of polarizability when there is no electromagnetic enhancement disturbance. Here, based on the molecular orientation sensitivity in GERS, an understanding of the chemical enhancement was promoted.

As shown in **Figure 5**a, when CuPc molecules make contact with graphene, interfacial dipoles form at the CuPc/graphene interface, which induces a change of the energy level of the CuPc molecules at the interface, especially the energy levels a_{1u} and e_g which are the orbitals for π-electron location.[40] Again, the formation of the interfacial electron states magnifies the available optical transition. Importantly, the magnitude of the polarizability, which governs

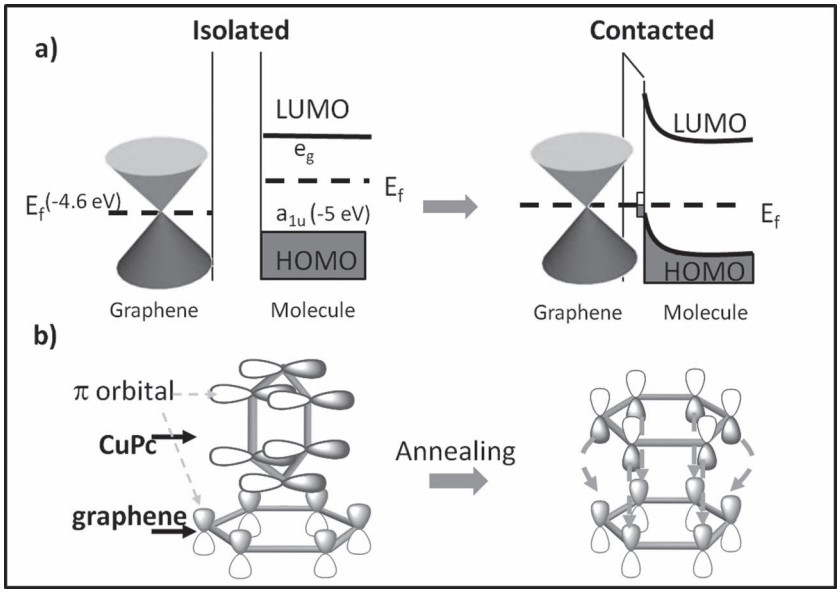

Figure 5. Understanding of the molecular orientation sensitivity in GERS. Schematic illustrations of a) the change of the electron energy band between graphene and the molecule before and after contact, and b) the relative direction of the delocalized π orbital of graphene and the CuPc molecule before and after annealing. E_f = Fermi level.

the magnitude of the Raman signal, depends explicitly on the available optical transition as Fermi's gold rule.[41] The Raman polarizability α can be expressed as:

$$\alpha = \left(\frac{2\pi}{\hbar}\right)\left|\sum_{n,n'}\frac{\langle i|H_{\text{light}}|n'\rangle\langle n'|H_{\text{el-ph}}|n\rangle\langle n|H_{\text{light}}|f\rangle}{(E_\lambda - E_{ii})(E_\lambda - E_{ii} - E_{\text{ph}})}\right|^2$$

where $|i\rangle$ is the initial state, $|n\rangle$ and $|n'\rangle$ are the two excited states in the Raman scattering process, $|f\rangle$ is the final state, H_{light} is the Hamiltonian of the light radiation, $H_{\text{el–ph}}$ is the Hamiltonian of the electron–phonon coupling, E_λ is the excited laser energy, E_{ii} is the electron transition energy, and E_{ph} is the phonon energy.[42] From the above equation, the Raman intensity depends on the strength of the electron–phonon coupling and resonance condition. Strictly speaking, resonance is only a sufficient condition for the enhancement, but not the necessary condition. Only if the polarizability is magnified will the Raman signals be enhanced. Hence, even though the absorption is decreased after annealing, as shown in Figure 3a, the Raman signals can be enhanced as shown in Figure 2a.

Since the energy level for the π electron locating in the CuPc molecule is close to that in graphene (for CuPc, the a_{1u} orbital is located at about –5 eV, and the Fermi level of graphene is about –4.6 eV),[36] the coupling of the π electrons in the CuPc molecule and graphene can be large at a certain molecular orientation. In this work, the different molecular orientations induce a different interfacial dipole, and then a different magnitude of polarizability. It should be noted that the magnitude of the interfacial dipole is dependent on both the density of the molecules and the molecular orientation.[17] For the lying-down orientation of CuPc molecules on graphene, the larger π–π interaction between the CuPc molecules and graphene induces a larger interfacial dipole, and then a larger Raman scattering cross section. In addition, when CuPc molecules adsorb on graphene in a lying-down orientation, the delocalized π-orbital cloud of the CuPc molecule overlaps more with that of graphene, as shown in Figure 5b. This indirectly provides the CuPc molecule with more opportunities for electron transition and then enhances the Raman scattering cross section of the CuPc molecule. Both the interfacial dipole and the overlap of the π-orbital cloud magnify the Hamiltonian of the electron–phonon coupling $H_{\text{el–ph}}$ and consequently the polarizability. This is the origin of the GERS molecular orientation sensitivity.

2.4. Quantitative Calculation of the CM Contribution Based on GERS and Evaluation of the Interaction between Graphene and the Molecule

Since the GERS system is perfect for simplifying the complex molecular orientation issue, quantitative calculation of the magnitude of the CM contribution can be implemented here. First, it should be noted that the magnitude of the CM contribution from the upstanding CuPc orientation to the lying-down CuPc orientation in Figure 2 is found to be vibrational mode dependent. **Table 1** summarizes the magnitude of the main Raman bands, the variation of their Raman shifts, and their assignments.[30,43] It clearly shows that not all the bands were magnified by the same amount, but were vibrational mode dependent. For example, for the vibration mode at 1530.8 cm^{-1}, the Raman intensity is enhanced about 10 times, while for the vibration mode at 483.8 cm^{-1} it becomes much weaker. This is consistent with the property of chemical enhancement, since different vibration modes behave differently in the enhancement "environment". The CuPc molecule is a square-planar molecule with D_{4h} symmetry. The Raman signals of CuPc

Table 1. Raman shift (P), Raman intensity (I), and the symmetry assignment of the Raman signals of CuPc LB film at room temperature (RT) and after annealing at 300 °C.

P_1(RT)	I_1(RT)	P_2(after annealing at 300 °C)	I_2(after annealing at 300 °C)	$P_2 - P_1$	I_2/I_1	Symmetry assignment and mode description
233.0	123.0	233.1	94.7	0.1	0.8	B_{2g}, macrocycle bending
255.3	48.9	256.2	41.9	0.9	0.9	A_{1g}, in-phase isoindole
483.8	368.0	483.2	153.7	–0.6	0.4	A_{2g}, out-of-plane pyrrole ring vibration
679.0	230.4	680.3	311.3	1.3	1.4	A_{1g}, macrocycle breathes symmetrically
747.2	261.3	746.9	561.9	–0.3	2.2	B_{1g}, deformation of the macrocycle
951.9	363.2	952.2	414.5	0.3	1.1	B_{2g}, specific deformation of the macrocycle
1106.1	240.1	1107.1	169.4	1.0	0.7	B_{1g}, antisymmetric vibration of the isoindole ring
1140.4	82.0	1141.6	494.5	1.1	6.0	B_{2g}, deformation of the isoindole ring
1307.0	324.5	1308.1	399.9	1.0	1.2	B_{1g}, antisymmetric vibration of the isoindole ring
1341.8	208.7	1341.9	1177.4	0.1	5.6	A_{1g}, symmetric vibration of the isoindole ring
1453.8	508.2	1452.4	1265.7	–1.4	2.5	B_{2g}, deformation of the isoindole ring system
1530.8	389.9	1530.7	4029.0	0.0	10.3	A_{1g}, symmetric stretching motion of isoindole groups
1581.7	70.1	1588.6	68.7	6.9	1.0	G band from graphene

small NANO MICRO

are mainly composed of two typical vibrations: one in the low-frequency area mainly originates from the macrocycle-related vibration; the other in the high-frequency area mainly originates from the isoindole-related vibration. Considering the relationship of the enhancement after molecular orientation change and the assignments of the vibration modes, the enhancement order can be deduced as: the isoindole ring vibration mode (e.g., 1530.8 cm^{-1}) > the macrocycle vibration mode (e.g., 679.0 cm^{-1}); the symmetric vibration mode (e.g., 1341.8 cm^{-1}) > the antisymmetric vibration mode (e.g., 1307.0 cm^{-1}); the out-of-plane vibration mode (e.g., 747.2 cm^{-1}) > the in-plane vibration mode (e.g., 679.0 cm^{-1}). This result not only indicates the change of the molecular orientation from upstanding to lying down, but also reflects that the isoindole ring is the main origin of the interaction between graphene and the CuPc molecule. The G-band shift of graphene indicates the charge transfer between graphene and the molecule, whereas the minimal change in the Raman band position of the CuPc Raman signals is indicative of only physical interaction between them. A more detailed analysis and explanation, with the assistance of multi-laser Raman measurements, will be reported elsewhere.

Next, to quantitatively calculate the magnitude of the CM contribution, the largest enhanced peak at 1530.8 cm^{-1} was used as reference, which was assigned to the symmetric stretching motion of all four isoindole groups.[30] By considering the change of the number of molecules and the Raman intensity, the magnitude of the CM contribution to the peak at 1530.8 cm^{-1} was calculated to be about 43 times. The calculation process is shown in Part 5 of the Supporting Information. Meanwhile, the same experiment was carried out for other planar Pc derivatives. A similar phenomenon was observed in the Raman spectra and UV–visible absorption spectra. The enhancement of the Raman signal for all of these Pc derivatives was observed after annealing. Moreover, the calculated magnitudes of the CM contribution are considerably different, which is consistent with the different interaction between graphene and these Pc derivatives. The detailed data are shown in Part 6 of the Supporting Information. Hence, no matter whether one examines the same molecule with different molecular orientations on graphene, or different molecules with the same orientation on graphene, the key point is that they have different dipole interaction with graphene, which is the origin of the different magnitudes of the CM contribution.

3. Conclusion

By making use of the properties of GERS ingeniously, this work promotes a rational approach to determine the molecular orientation sensitivity of chemical enhancement. It is promising to use GERS for detecting the molecular orientation on graphene, as well as the interaction between graphene and the molecules. Furthermore, an understanding of the chemical enhancement in GERS was promoted and the effect of molecular orientation on the intensity of chemical enhancement could be well explained.

4. Experimental Section

CuPc and other Pc derivatives were dissolved in a mixture of trifluoroacetic acid and dichloromethane [1:10 (v/v)] to prepare spreading solutions. Concentrations of Pc derivatives in the sample solutions were of the order of 2×10^{-4} M (mol L^{-1}). The monolayer Pc derivative LB films were obtained on a LB trough (NIMA Technology, Type: 611, Serial No. 093) with a constant pressure of 20 mN m^{-1} and by the horizontal dipping method in a speed range of 2 mm min^{-1}.

Raman spectra were collected using a Horiba-Jobin Yvon Labram HR800 instrument with a 632.8 nm He–Ne laser. A 100× objective was used to focus the laser beam. The laser power was controlled below 1 mW to avoid the decomposition of molecules and the heating effect. The exposure time was 2 s. The spectra for the comparison were obtained under the same conditions. The intensities of the peaks were obtained by fitting them with a Lorentzian function. The UV–visible absorption spectra were collected on a Perkin–Elmer Lambda-950 UV/Vis/near-IR spectrophotometer. The transmission mode was used. The quartz substrate for the measurements was highly transparent (>95%) in the UV–visible region. AFM images were obtained on a Veeco NanoScope IIIA instrument in the tapping mode.

Supporting Information

Supporting Information is available from the Wiley Online Library or from the author.

Acknowledgements

This work was supported by the NSFC (20673004, 20725307, and 50821061), MOST (2006CB932701, 2006CB932403, and 2007CB936203), and "The Fundamental Research Funds for the Central Universities".

[1] M. Orrit, P. Tamarat, A. Maali, B. Lounis, *J. Phys. Chem. A* **2000**, *104*, 1–16.
[2] S. M. Nie, S. R. Emory, *Science* **1997**, *275*, 1102–1106.
[3] B. Ren, X. M. Lin, Y. Cui, Y. H. Xu, Z. Q. Tian, *Anal. Bioanal. Chem.* **2009**, *394*, 1729–1745.
[4] G. C. Schatz, M. A. Young, R. P. Van Duyne, *Top. Appl. Phys.* **2006**, *103*, 19–45.
[5] M. E. Lippitsch, *Phys. Rev. B* **1984**, *29*, 3101–3110.
[6] F. J. Adrian, *J. Chem. Phys.* **1982**, *77*, 5302–5314.
[7] A. Otto, M. Futamata, *Top. Appl. Phys.* **2006**, *103*, 147–182.
[8] H. X. Xu, J. Aizpurua, M. Kall, P. Apell, *Phys. Rev. E* **2000**, *62*, 4318–4324.
[9] A. Campion, P. Kambhampati, C. M. Child, M. C. Foster, *J. Chem. Phys.* **1998**, *108*, 5013–5026.
[10] L. Jensen, S. M. Morton, *J. Am. Chem. Soc.* **2009**, *131*, 4090–4098.
[11] X. Ling, L. M. Xie, Y. Fang, H. Xu, H. L. Zhang, J. Kong, M. S. Dresselhaus, J. Zhang, Z. F. Liu, *Nano Lett.* **2010**, *10*, 553–561.

[12] X. Ling, J. Zhang, *Small* **2010**, *6*, 2020–2025.
[13] H. Xu, L. M. Xie, H. L. Zhang, J. Zhang, *ACS Nano* **2011**, *5*, 5338–5344.
[14] H. Xu, Y. B. Chen, W. G. Xu, H. L. Zhang, J. Kong, M. S. Dresselhaus, J. Zhang, *Small* **2011**, *7*, 2945.
[15] E. C. L. Ru, P. G. Etchegoin, *The Principle of Surface-Enhanced Raman Spectroscopy*, Elsevier, Oxford **2009**, Ch. 4, pp. 192–197.
[16] B. G. Janesko, G. E. Scuseria, *J. Phys. Chem. C* **2009**, *113*, 9445–9449.
[17] K. I. Ikeda, K. S. Suzuki, K. Uosaki, *Nano Lett.* **2011**, *11*, 1716–1722.
[18] L. J. Guo, J. J. Yu, Y. C. Li, Y. Z. Gu, Y. B. Huang, Y. J. Mo, *Chin. Sci. Bull.* **2000**, *45*, 1464–1467.
[19] A. G. Brolo, Z. Jiang, D. E. Irish, *J. Electroanal. Chem.* **2003**, *547*, 163–172.
[20] E. C. Le Ru, P. G. Etchegoin, *Phys. Chem. Chem. Phys.* **2008**, *10*, 6079–6089.
[21] P. G. Etchegoin, C. Galloway, E. C. Le Ru, *Phys. Chem. Chem. Phys.* **2006**, *8*, 2624–2628.
[22] E. C. Le Ru, J. Grand, N. Felidj, J. Aubard, G. Levi, A. Hohenau, J. R. Krenn, E. Blackie, P. G. Etchegoin, *J. Phys. Chem. C* **2008**, *112*, 8117–8121.
[23] L. Brus, A. M. Michaels, J. Jiang, *J. Phys. Chem. B* **2000**, *104*, 11965–11971.
[24] G. Haran, T. O. Shegai, *J. Phys. Chem. B* **2006**, *110*, 2459–2461.
[25] K. S. Novoselov, A. K. Geim, S. V. Morozov, D. Jiang, Y. Zhang, S. V. Dubonos, I. V. Grigorieva, A. A. Firsov, *Science* **2004**, *306*, 666–669.
[26] K. Ogawa, H. Yonehara, C. J. Pac, *Langmuir* **1994**, *10*, 2068–2070.
[27] K. Xiao, Y. Q. Liu, X. B. Huang, Y. Xu, G. Yu, D. B. Zhu, *J. Phys. Chem. B* **2003**, *107*, 9226–9230.
[28] C. Wang, S. X. Yin, B. Xu, C. L. Bai, *J. Phys. Chem. B* **2002**, *106*, 9044–9047.
[29] D. M. Guldi, J. Malig, N. Jux, D. Kiessling, J. J. Cid, P. Vazquez, T. Torres, *Angew. Chem. Int. Ed.* **2011**, *50*, 3561–3565.
[30] A. J. Bovill, A. A. Mcconnell, J. A. Nimmo, W. E. Smith, *J. Phys. Chem.* **1986**, *90*, 569–575.
[31] U. Salzner, *J. Phys. Chem. A* **2008**, *112*, 5458–5466.
[32] A. A. M. Farag, *Optics Laser Technol.* **2007**, *39*, 728–732.
[33] H. Q. Xiang, K. Tanaka, T. Kajiyama, *Langmuir* **2002**, *18*, 9102–9105.
[34] H. Q. Xiang, K. Tanaka, A. Takahara, T. Kajiyama, *Langmuir* **2002**, *18*, 2223–2228.
[35] L. Colombo, X. S. Li, W. W. Cai, J. H. An, S. Kim, J. Nah, D. X. Yang, R. Piner, A. Velamakanni, I. Jung, E. Tutuc, S. K. Banerjee, R. S. Ruoff, *Science* **2009**, *324*, 1312–1314.
[36] M. S. Liao, S. Scheiner, *J. Comput. Chem.* **2002**, *23*, 1391–1403.
[37] M. Szybowicz, W. Bala, K. Fabisiak, K. Paprocki, M. Drozdowski, *J. Mater. Sci.* **2011**, *46*, 6589–6595.
[38] R. Prabakaran, R. Kesavamoorthy, G. L. N. Reddy, F. P. Xavier, *Phys. Status Solidi B* **2002**, *229*, 1175–1184.
[39] G. Q. Shi, H. Bai, C. Li, *Adv. Mater.* **2011**, *23*, 1089–1115.
[40] W. D. Dou, S. P. Huang, R. Q. Zhang, C. S. Lee, *J. Chem. Phys.* **2011**, *134*, 094705.
[41] E. C. L. Ru, P. G. Etchegoin, *The Principle of Surface-Enhanced Raman Spectroscopy*, Elsevier, Oxford **2009**, Ch. 4, pp. 258–261.
[42] W. L. Peticolas, L. Nafie, P. Stein, B. Fanconi, *J. Chem. Phys.* **1970**, *52*, 1576–1584.
[43] J. Z. Jiang, Z. Q. Liu, X. X. Zhang, Y. X. Zhang, *Spectrochim. Acta A* **2007**, *67*, 1232–1246.

Received: October 21, 2011
Revised: December 9, 2011
Published online: February 23, 2012

